CHAPTER VII
RHEOLOGICAL PROPERTIES OF POLYPYRROLE NANOPARTICLES/ALGINATE SUSPENSION

7.1 Abstract

Rheological behaviors of polypyrrole (PPY) nanoparticles suspended in alginate were investigated, compared to those of the macroscopic counterpart. Monodisperse PPY nanoparticles with spherical in shape were synthesized by oxidative polymerization of pyrrole in the presence of carboxymethyl chitin (CM-chitin) template. CM-chitin template was subsequently removed by simply washing with distilled water. Different sizes of PPY nanoparticles were achieved by varying concentration of CM-chitin. Contrary, large size aggregated PPY macroparticles was obtained by conventional route (without the addition of template). FTIR indicates an identical structure of the conventional PPY macroparticles and the PPY nanoparticles. Rheological study shows a different in rheological behaviors of PPY macroparticles and PPY nanoparticles suspended in alginate solution. The addition of PPY macroparticles increased the viscosity of alginate, while the decrease of viscosity of alginate was observed by adding PPY nanoparticles. The decrease of viscosity is attributed to the depletion of alginate concentration in bulk medium due to the absorption of alginate molecules on the surfaces of PPY nanoparticles combining with the stabilization of alginate-absorbed PPY nanoparticles, hence reduces the chain entanglements of alginate molecules and prevent the aggregation of PPY nanoparticles. Dynamic light scattering suggests the absorption of alginate molecules on to surface of PPY nanoparticles. The influences of PPY particle sizes and electronic states on the rheological behaviors of PPY/alginate suspensions are explored.

7.2 Introduction

Alginate is an anionic polysaccharide consisting of 1,4-linked β-D mannuronic (M) and α-L gluluronic (G) acid residuals produced by brown algae and

some bacteria (Gombotz and Wee 1998; Lattner *et al.* 2003). There are three different types of block copolymer that made up of M-block, G-block, and MG-block. The sequence of block types is highly dependent on the source of alginate (Chen *et al.* 2006). It is well known that alginate forms hydrogel via a complex between divalence cations, except Mg^{2+}, and G-block of two alginate polymers resembling egg-box structure (Liu *et al.* 2003). Alginate is widely applicable in biomedical and pharmaceutical applications (Kabu *et al.* 2003; Sriamornsak *et al.* 2007). Moreover, due to the ability to form shape, especially in films and fibers, alginate has been used as a matrix in the preparation of composite materials (Bhat *et al.* 2006; Watthanaphanit *et al.* 2008).

Polypyrrole (PPY) is one of the most extensively study conductive polymers due to its facile synthesis by chemical or electrochemical process, good environmental stability, easy conductivity control, and low cost of monomer (Salmon *et al.* 1982; Chen *et al.* 1993; Okuzaki *et al.* 1999). PPY has been used in fuel cells, electrochromic displays, sensors, actuator and even artificial muscles (Peter *et al.* 1996; Pernaut and Reynolds 2000; Paitan *et al.* 2003). However, the mentioned application has been hampered due to their poor processability and mechanical properties. These drawbacks can be improved by the fabrication of composite materials.

Recently, the composite materials consisting of conductive polymer and hydrogel have great attracted interest. The combination of these components can produce an electroactive hydrogel which enable physical and/or chemical transitions in response to electrical stimulus (Thanpitcha *et al.* 2006). The electroactive hydrogel is potentially used in the applications of biosensors (Abu-Rabeah and Marks 2009; Brahim *et al.* 2002), nerve regenerations (Kotwal and Schmidt 2001), artificial muscles (Ismail *et al.* 2008; 2009), and electrically controlled release (Small *et al.* 1997; Niamlang and Sirivat *in press*). However, to fabricate this type of the composite materials, the rheological behaviors of the composites in molten state have to be considered in order to gain beneficial data for designing the polymer processing and predicting the product properties (Krishnamoorti and Yurekli 2001). The rheological behaviors of particulate suspension were first explored by Einstein who demonstrated that the viscosity of suspension normally increases as a function of

particle volume fraction and the viscosity of suspending liquid (Einstein 1906). Additionally, suspension of particles in polymeric liquids produces a similar increase in viscosity (Metzner 1985). However, not only the presence but the distribution of particles also influences the rheological behaviors and the product properties of the obtained composite materials (Dangtangee *et al.* 2005). It is widely recognized that the distribution of particles in polymeric liquids is governed by the interplay between the inter-particle interaction and particles-polymer interaction (Chen *et al.* 2007).

When incorporated particles in polymeric liquids, the polymer chains can absorb onto the surfaces of particles and render the stabilization (well distribution) or aggregation (poor distribution) accompanied with changes in the microstructures of the particles (Chen *et al.* 2007; Doi *et al.* 2002; He and Zhao 2007). A prevalence of stabilization over aggregation of particles is generally considered in obtaining suspensions of low viscosity. Shen et al. stated that the stabilization of particles in media occurred from the electrostatic repulsion, or steric repulsion, or the combination of both, called electrosteric repulsion (Shen *et al.* 2004). In addition, a surface treatment of particles with dispersants or polyelectrolytes apparently improves the distribution of particles due to the enhancement of the particles-polymer interaction.

Reduction in size of the particles to nano-scale may be another way that enhances the distribution of particles in the polymeric liquids due to the excessive surface contact area of particles to the media (Li *et al.* 2007). Interestingly, Mackay et al. found that the incorporation of crosslinked PS nanoparticles could reduce the viscosity of PS melt due to the enhancement of free volume introduced by the presence of the nanoparticles while an increase of viscosity was clearly observed when incorporated crosslinked PS macroparticles (Mackay *et al.* 2003). However, to our best knowledge, there was lack of systemic investigation on the different rheological behaviors of macro and nanoparticles of conductive polymer suspended in polymer solution.

In this present work, we highlight on the rheological characterization of the macroparticles and nanoparticles of PPY suspended in alginate solution. The spherical PPY nanoparticles with narrow size distribution were synthesized by using self-assemble carboxymethyl chitin (CM-chitin) as a template, similar to the method

described by our previous work (Thanpitcha *et al.* 2008). The different sizes of PPY nanoparticles were obtained by varying the template concentration. Contrary, the large irregularly shape PPY aggregate with a diameter in range of micrometer was obtained by conventional method (without the addition of template). The effects of particle size and electronic states of PPY nanoparticles on rheological properties of the suspensions are also discussed.

7.3 Experimental

7.3.1 Materials

Pyrrole was purchased from Aldrich and was distilled under reduced pressure prior to use. AR grade ammoniumperoxodisulfate (APS) was purchased from Merck.

Chitin, with a degree of deacetylation (%DD) equal to 20%, measured by the method of Baxter *et al.*, (Baxter *et al.* 1992) was prepared from shrimp shell (*Penaeus merguiensis*), kindly supplied by Surapon Food Co. Ltd, Thailand. AR grade hydrochloric acid, sodium hydroxide, tetrahydrofuran (THF), and acetone were purchased from Fisher Sciencetific and used as received. Alginate was purchased from Calro. AR grade monochloroacetic acid was purchased from Acros Organics.

7.3.2 Preparation of Carboxymethyl Chitin (CM-chitin)

CM-chitin, with a degree of substitution (DS) equal to 0.43, was prepared by the reaction of chitin powder with monochloroacetic acid under basic conditions according to the method described by Wongpanit (Wongpanit *et al.* 2005). In a typical procedure, CM-chitin was prepared by suspending 5 g of chitin powder in 100 g of 42 %w/w NaOH. The suspension was stored under reduced pressure for 30 min. Then, 160 g of crushed ice was added to the suspension and the mixture was stirred at below 5°C for 30 min. A pre-cooled solution at a temperature below 5°C, containing 27 g monochloroacetic acid in 70 ml of 14% w/w NaOH, was slowly added to the mixture with vigorous stirring. The reaction was maintained at 0-5°C for 30 min. After settling at room temperature overnight, the mixture was neutralized with glacial acetic acid and subsequently dialyzed in running water, followed by

dialysis with distilled water for 1 day. The dialysate was centrifuged at 10,000 rpm for 20 min to remove the insoluble material. A white solid was recovered from the supernatant by adding it drop-wise into acetone. The product was washed with ethanol, filtered, and dried in a vacuum at room temperature.

7.3.3 Synthesis of Polypyrrole Nanoparticles by using CM-chitin as a Template

PPY nanoparticles (nPPY) in a doped state were synthesized in aqueous solution by the oxidative polymerization of pyrrole, using APS as an oxidant, in the presence of CM-chitin, acting as a template. The synthesis procedure is described as follows: 8 g of pyrrole monomer was poured into 50 g of aqueous CM-chitin solutions (at concentrations of 0.5 wt%, 1 wt%, or 2 wt%) and the mixture was cooled to 0°C with mechanical stirring at 300 rpm for 1 h. 100 ml of 1.5-M HCl was added drop-wise into the mixture within 30 min and the solution was maintained with mechanical stirring for 30 min. Next, a pre-cooled solution, at a temperature below 5°C, containing 10 g (0.048 mole) APS in 100 ml of 1.5-M HCl was added drop-wise within 30 min, and the reaction was stirred at 0°C for 4 h to complete the polymerization. The suspension was dialyzed with an excess amount of distilled water for 2 days in order to neutralize suspension and remove of CM-chitin template. Subsequently, the suspension was centrifuged at 11,000 rpm for 20 min. The precipitated product was re-dispersed in 100 ml THF, sonicated for 30 min, evaporated out the solvent, and kept in desiccators prior to use.

In addition, the conventional PPY macroparticles (CPPY) in the doped state was synthesized in a similar procedure but without the addition of CM-chitin template.

7.3.4 Preparation of Polypyrrole/Alginate Suspension

PPY powders (both the synthesized nPPY and CPPY) were firstly dispersed in distilled water and sonicated for 30 min to obtain the well dispersed PPY suspensions. The appropriate amount of alginate was added into the PPY suspensions in order to achieve a certain amount of PPY to alginate; those are 10, 20, 30, 40, and 50 wt%. Subsequently, the prepared suspensions were magnetically

stirred at 400 rpm for 12 h in order to complete the dissolution of alginate and obtain the homogeneous PPY/alginate suspensions.

7.3.5 Characterization

FTIR spectra were recorded using a Thermo Nicolet Nexus 670 FTIR spectrometer in the absorbance mode at 32 scans with a resolution of 4 cm^{-1}. Spectra in the frequency range of 4,000-400 cm^{-1} were measured using a deuterated triglycerinesulfate detector (DTGS) with a specific detectivity of 1×10^9 $cm \cdot Hz^{1/2} \cdot w^{-1}$.

The morphologies of the synthesized nPPY and CPPY were investigated using a scanning electron microscope (JOEL, model JSM-5800LV) at 15 kV. Samples were prepared by the dispersion of PPY powders in distilled water, sonicating for 5 min, and placing a drop onto a brass stub before gold sputtering.

Steady and oscillatory shear measurements of neat alginate and the PPY/alginate suspensions were carried out on a strain controlled TA Instruments AR 2000ex Rheometer. A cone-and-plate geometry with a diameter of 40 mm and a cone angle of 2° was used for all determinations. The instrument was equipped with a solvent trap to prevent water evaporation. All rheological measurements were conducted at a temperature of 25 °C and within two days after preparing the suspensions in order to avoid the appearance of any time dependent transitions in the suspensions. Prior to test, an oscillating pre-sheared at angular frequency of 30 rad/s under the controlled strain of 500% was performed for 10 min followed by a time sweep at angular frequency of 6.283 rad/s under the controlled strain of 0.2% for 10 min. Such pre-conditionings allowed us to erase previous shear history on the samples. Steady shear experiment was performed over shear rate range of 0.1 to 100 s^{-1}, while the oscillatory shear experiment was carried out over angular frequency range of 0.1 to 100 rad/s under the controlled strain of 0.2%. Both shear viscosity and moduli (G′, G″) measurements were repeated duplicated or triplicate to confirm reproducibility.

Dynamic light scattering was used to determine hydrodynamic radius of the synthesized PPY nanoparticles as well as the PPY nanoparticles/alginate suspensions at a detection angle of 90° with a Brookhaven instrument, equipped with

a 15 mW He - Ne laser emitting vertically polarized light at wavelength 632.8 nm. The measurements were carried out at 25°C on highly diluted samples (0.001 mg/ml) in order to rule out interaction and multiple scattering effects. Prior to the test, all samples were filtered through the filter with pore size of 450 nm. The average diameter was computed from the autocorrelation function data by using the cumulant analysis method.

7.4 Results and Discussion

7.4.1 Morphology of Polypyrrole Nanoparticles and Possible Mechanism

The morphology of nPPY synthesized in the presence of CM-chitin, acting as a template, were illustrated by SEM images in comparison to that of CPPY, synthesized without the addition of CM-chitin template, as shown in Figure 7.1. It was observed that the CPPY has large irregularly shaped aggregates with an average diameter greater than 500 nm (Fig. 7.1a). By the addition of 0.25 wt% CM-chitin solution (025CMCT) into the polymerization media, the synthesized PPY has a reasonably monodisperse spherical morphology with an average diameter of 217 ± 17 (Fig. 7.1b).

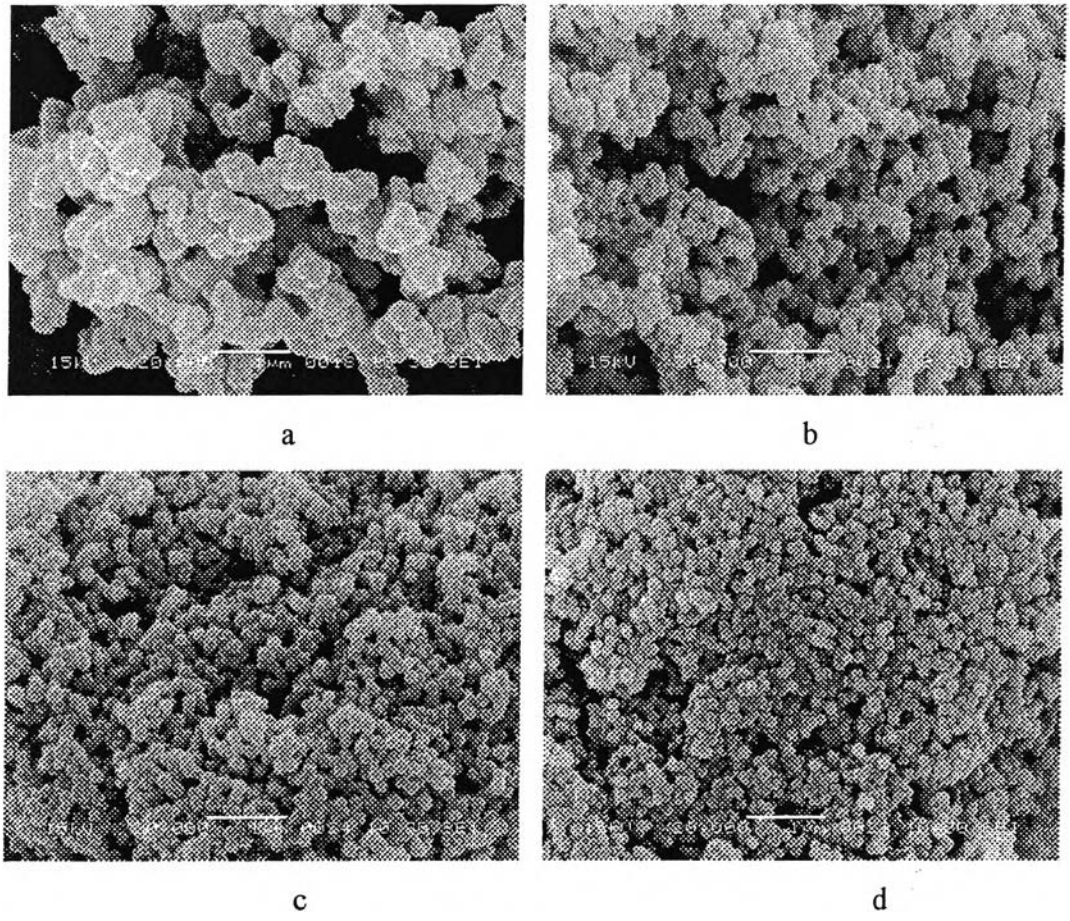

Figure 7.1 SEM images of CPPY and nPPY (synthesized in the presence of different CM-chitin concentrations) after washing with distilled water: a) CPPY, b) nPPY-(025CMCT), c) nPPY-(05CMCT), and d) nPPY-(1CMCT).

The explanation and formation mechanism of the obtained nPPY is proposed based on a self-assembly process of CM-chitin. From our previous work, we reported that CM-chitin can self-assemble and forms core-shell structure, acting as a template, (Thanpitcha *et al.* 2008) due to its amphiphilic character with equatorial hydrophilic edges (-OH, NH_3^+, $-OCH_2COOH$, and $-NHCOCH_3$) oriented toward exterior aqueous phase to form hydrophilic shell, and axial hydrophobic planes (C-H bond in glucopyranose unit), orient towards the interior to form the hydrophobic core (Ueno *et al.* 2007). Under acidic conditions for PPY synthesis, the equatorial hydrophilic edges can form hydrogen bonding and/or electrostatic interaction with the protonated nitrogen of protonated pyrrole molecules, while axial

hydrophobic planes can strongly interact with the sp^2 hybridized orbital of aromatic rings of the protonated pyrrole molecules due to CH-π bonding (Palma *et al.* 2000). This leads to the immigration of pyrrole into core-shell structure of CM-chitin and it subsequently formed nucleating sites at the interface of core-shell structure. After adding APS, the oxidizing agent, the protonated pyrrole was initiated and subsequently polymerized within the core-shell structure of CM-chitin to form spherical shaped nPPY with a narrow size distribution. However, it was found that the size of the obtained nanoparticles was influenced by concentration of CM-chitin template. By increasing the concentration of CM-chitin template from 0.25 (025CMCT), to 0.5 (05CMCT), and 1 wt% (1CMCT), the size of the obtained nPPY was decreased from 217 ± 17 nm (Fig. 7.1b), to 178 ± 12 nm (Fig. 7.1c), and 136 ± 14 nm (Fig. 7.1d), respectively. This result seems reasonable, because the increase of CM-chitin concentration increases the number of nucleating sites (Stejskal and Sapurina 2004). Since a higher number of nucleating sites leads to a lower amount of monomer uptake in each hydrophobic core, the result is a decrease in size of the nPPY.

To compare the dispersion behavior between the synthesized nPPY-(025CMCT) and CPPY, cross-sectional morphology of the composite films consisting of the synthesized nPPY-(025CMCT) and CPPY dispersed in CM-chitin matrix were investigated as shown in Figure 7.2. CM-chitin was used as the matrix in this experiment for eliminating the influence of the remaining CM-chitin in the nPPY-(025CMCT) in case of CM-chitin template could not be completely removed from the synthesized nPPY-(025CMCT). Figure 7.2a shows the homogenous cross-sectional surface of neat CM-chitin. By adding 10 wt% CPPY into CM-chitin matrix, the distinct aggregated CPPY is clearly observed (Fig. 7.2b). In addition, the film can not be fabricated when further increase the loading content of CPPY into the CM-chitin matrix due to extensive phase separation and film brittleness (Figure 7.2c). Contrary, nPPY-(025CMCT) were well dispersed thoroughly in CM-chitin matrix and there was no a distinct aggregation or phase separation observed even increase of nPPY-(025CMCT) content up to 50 wt% (Fig. 7.2d). This implies that the smaller size of PPY nanoparticles provide a better dispersion in the CM-chitin matrix than

that of CPPY. In addition, it was further observed that the morphology of nPPY-(025CMCT) still retains when incorporating into CM-chitin matrix.

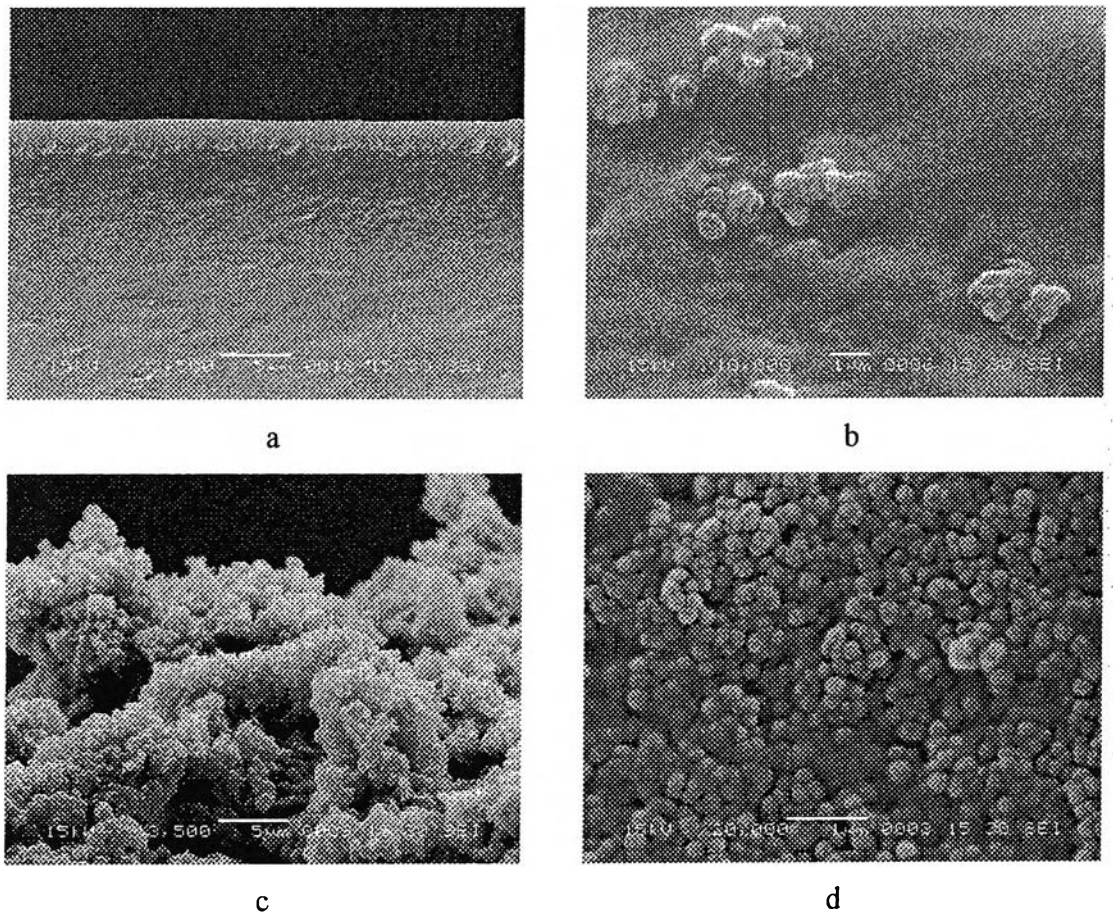

Figure 7.2 Cross-sectional morphologies of PPY/CM-chitin composite films: a) CM-chitin; b) 10 wt% CPPY/CM-chitin; c) 50 wt% CPPY/CM-chitin; and d) 50 wt% nPPY-(025CMCT)/CM-chitin.

7.4.2 FTIR Spectra of Polypyrrole Nanoparticles

The chemical structures of acid form of CM-chitin, used as a template, CPPY, and the synthesized nPPY-(025CMCT) were characterized by FTIR spectra as shown in Figure 7.3. The characteristic peaks of acid form of CM-chitin, occurring under acidic conditions for the polymerization of pyrrole, arise at 1743, 1650, 1379, and 1067 cm^{-1} corresponding to COOH stretching, asymmetric C=O, symmetric C=O stretching, and C-O-C stretching of pyranose ring, respectively, (Mi

et al. 1997) (Fig. 7.3a). After polymerization of pyrrole and subsequent removal of the CM-chitin template by washing with distilled water, the characteristic peaks of nPPY-(025CMCT), observed at 1553, 1466, 1306, and 1195 cm^{-1} were attributed to C=C stretching, C-C stretching, C-H in-plane, and C-N stretching vibration, respectively (Liu *et al.* 2006) (Fig. 7.3c). These characteristic peaks were consistent with FTIR spectrum of CPPY in doped state (Fig. 7.3b). However, the characteristic peaks of CM-chitin template could not be observed in the FTIR spectra of the nPPY-(025CMCT) synthesized in the presence of CM-chitin after washing with distilled water (see Fig. 7.3c). This indicates the complete removal of CM-chitin template by simply washing with distilled water.

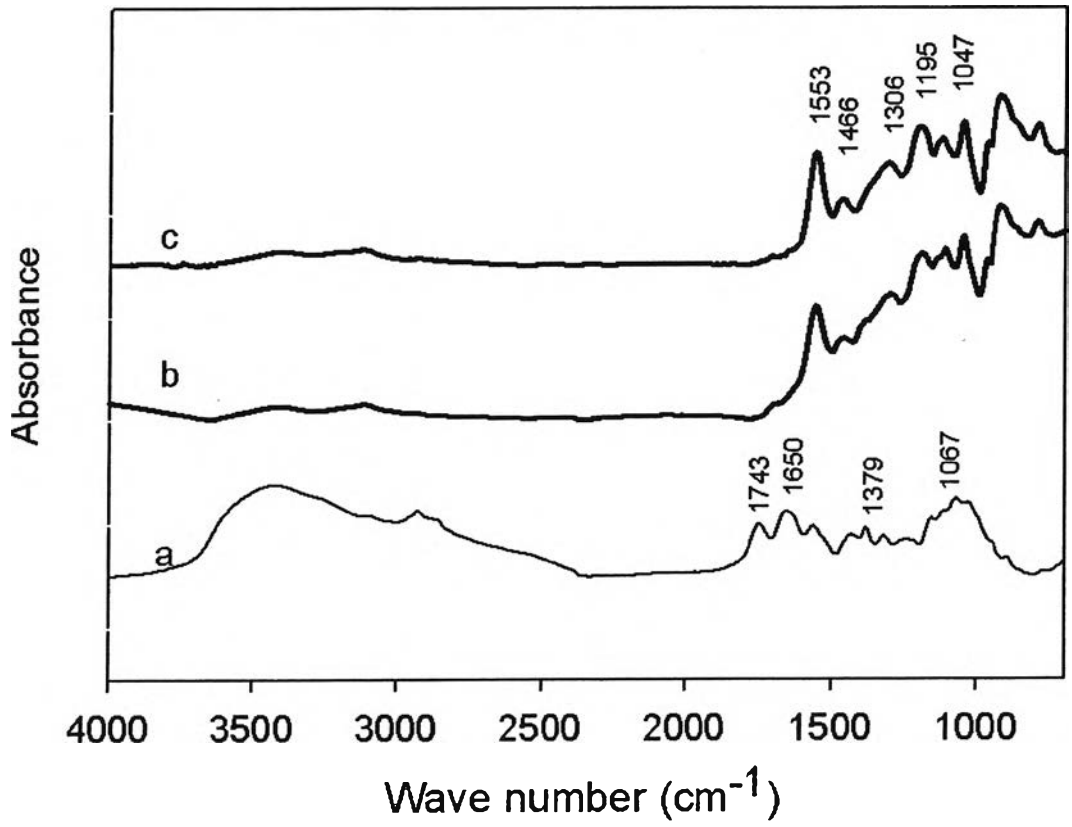

Figure 7.3 FTIR spectra of a) CM-chitin (acid form); b) CPPY; c) nPPY-(025CMCT).

7.4.3 Rheological Behaviors of Polypyrrole/Alginate Suspensions

7.4.3.1 Effect of Blend Composition

Figure 7.4 shows flow curves for both steady shear and oscillatory shear measurements of neat 4 wt% alginate and different contents of doped CPPY suspended in 4 wt% alginate solution. The dependence of shear viscosity on shear rate is shown in Figure 7.4a. Evidently, within the shear rate range examined (0.1-100 s^{-1}), neat alginate exhibits a Newtonian behavior (viscosity is nearly independence of shear rate), at low shear rate (about 0.1-1 s^{-1}), while, at higher shear rate (about 1-100 s^{-1}), shear viscosity decreases with increasing shear rate. Fluids that display this behavior are termed shear-thinning. The molecular basis for shear-thinning behavior is the effect of shear on entanglements of the polymer matrix. At low shear rate, the entanglements impede shear flow and, therefore, viscosity is high. As shear rate increases, chain begin to orient in the flow direction and disentangle from one another, consequently, the viscosity begins to drop. However, the formation of new entanglement may be occurred at the same time of disentanglements, particularly at high concentrated solution. Therefore, the shear thinning behavior in concentrated solution may ascribed by the greater rate of disruption of entanglements than that of the formation of new entanglements (Xu *et al.* 2009).

By incorporating the doped CPPY into alginate, the CPPY/alginate suspensions show a similar flow curve with neat alginate but the shear viscosity of CPPY/alginate suspension is higher than that of neat alginate. Generally, the addition of particles in polymeric liquids leads to an increase in the viscosity because the presence of such particles obstructs shear flow. Moreover, the shear viscosity of CPPY/alginate suspensions apparently increases with increasing CPPY content. The suspension viscosity revealed a pronounced increase in inter-particles interactions when the solid loading was increased. Therefore, it is believed that, an aggregation of CPPY become more dominant with increase of CPPY content due to the enhancement of an inter-particle attractive force, such as the van der Waal attraction and/or the electrostatic interaction (Chen *et al.* 2007). The aggregated CPPY particles usually result in a significant increase in suspension viscosity.

Figure 7.4b shows the dependence of storage (G′) and loss moduli (G″) on angular frequency of neat alginate and CPPY/alginate suspensions. For all alginate and their blend samples, G″ is higher than G′. This type of properties is typical of solution that exhibits a dominant viscous behavior. The G′ and G″ are strongly dependent on both the frequency and amount of CPPY loading. Both G′ and G″ increase with increasing frequency as well as increasing CPPY content. As shown in Fig. 7.4b, the values of G′ of the suspensions, however, significantly increases with increasing CPPY loading at low frequencies and got close together at a high frequency range. This is because high frequency region relates with the motion of the particles. The inter-particle interaction that leads to the increasing of the values of G′ may contribute less in this frequency region. Therefore, the effect of the CPPY content is much more notable at low frequencies than at high frequencies (Liu and Chen 2008). Moreover, at high CPPY content, particularly at 30 to 50 wt% CPPY content, the narrow frequency independence of G′ at low frequency regime is observed corresponding to a pseudo-solid-like behavior, and indicating a formation of percolating particle network. (Sarvestani 2008). Additionally, the complex viscosity versus angular frequency curve (see Fig. 7.4c) for the suspensions has a similar tendency with the shear viscosity described above.

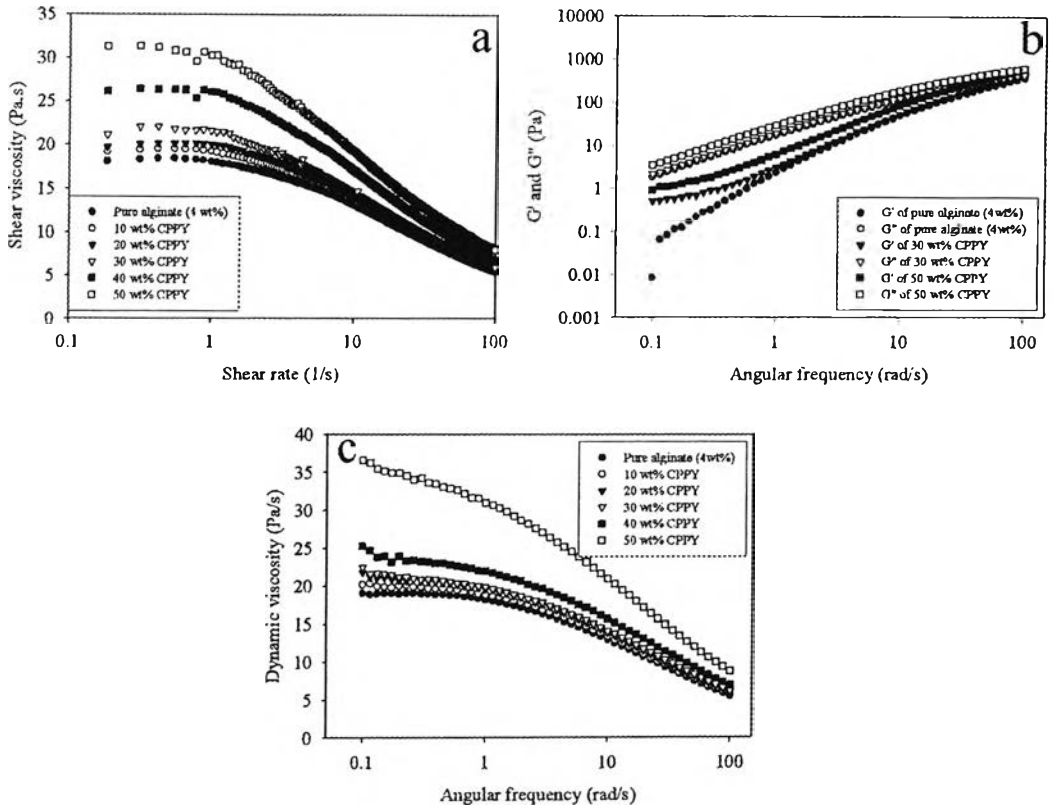

Figure 7.4 Steady shear and oscillatory shear measurements of doped CPPY suspended in 4 wt% alginate solution: a) plot of shear viscosity against shear rate; b) plot of storage (G') and loss (G") moduli against angular frequency; and c) plot of dynamic viscosity against angular frequency.

To explore the different in rheological behaviors of the doped CPPY and the doped nPPY suspended in 4 wt% alginate solution, the doped nPPY-(025CMCT) with the average diameter of 217 nm (determined from SEM measurement), were used in this study. By adding the doped nPPY-(025CMCT) into 4 wt% alginate, it was surprisingly found that the shear viscosity of suspensions gradually decreases from neat alginate to the minimum value at 20 wt% doped nPPY-(025CMCT) content, and followed by slightly increase when further increase doped nPPY-(025CMCT) content up to 50 wt% as shown in Figure 7.5a. However, the shear viscosity of 50 wt% doped nPPY-(025CMCT) suspended in 4 wt% alginate is still lower than that of neat 4 wt% alginate. The decreasing in shear viscosity of doped nPPY-(025CMCT)/alginate suspensions is attributed to the depletion of

alginate concentration in a bulk suspension medium. Basically, when suspended the positive charge of doped nPPY-(025CMCT) into the negative charge alginate, the absorption of alginate molecules onto the surface of doped nPPY-(025CMCT) occurs due to an electrostatic interaction between two opposite charges (Kawakami *et al.* 2001). The absorption of alginate on the doped nPPY-(025CMCT) surfaces possibly reduces the alginate concentration of the bulk medium, hence decreases in the entanglement of alginate molecules. This results in the lowering in shear viscosity of the doped nPPY-(025CMCT)/alginate suspensions, compared to that of neat alginate.

Moreover, the alginate-absorbed nPPY-(025CMCT) possibly hampers the aggregation of such particles in the alginate matrix due to their electrostatic repulsion arising from the repellent of like-charged alginate-absorbed nPPY-(025CMCT) or the steric repulsion between nPPY-(025CMCT) surfaces coated with alginate molecules, or by the structural contributions from independent, non-adsorbing alginate solutions (Tiller and O'Melia 1993; Stenkamp *et al.* 2001). Therefore, the decrease of shear viscosity was observed when increasing nPPY-(025CMCT) up to 20 wt%. However, the aggregation of the doped nPPY-(025CMCT) became more dominant due to the favorable inter-particles attraction when further increased the doped nPPY-(025CMCT) content from 20 wt% to 50 wt%. This directly results in the increase of shear viscosity of the suspensions.

The storage and loss moduli dependent on angular frequency for the doped nPPY-(025CMCT)/alginate suspensions exhibit relative results likely observed in shear viscosity (see Fig. 7.5b). The values of storage and loss moduli decrease from the neat alginate when adding the nPPY-(025CMCT) content up to 20 wt% and then turn increase with further increase of nPPY-(025CMCT) content. However, the moduli of all nPPY-(025CMCT)/alginate suspensions are lower than that observed in neat alginate. In contrast to CPPY/alginate suspension, the frequency independence of G′ at low frequency regime disappears in the nPPY-(025CMCT)/alginate suspensions. This suggests that particle network may not be formed when adding the doped nPPY-(025CMCT) into alginate.

Again, dynamic viscosity of different content of the doped nPPY-(025CMCT) suspended in 4 wt% alginate (see Fig. 7.5c) reveals a similar tendency with shear viscosity.

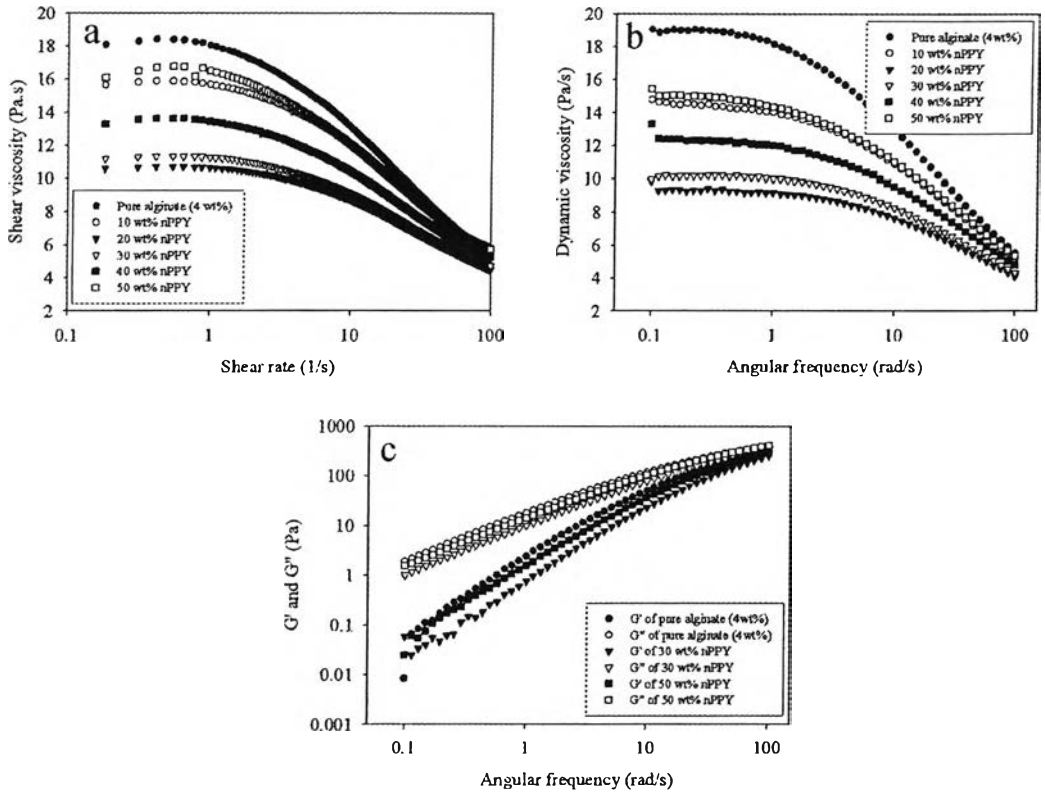

Figure 7.5 Steady shear and oscillatory shear measurements of the doped nPPY-(025CMCT) suspended in 4 wt% alginate solution: a) plot of shear viscosity against shear rate; b) plot of dynamic viscosity against angular frequency; and c) plot of storage (G') and loss (G") moduli against angular frequency.

7.4.3.2 Effect of Particle Size of Polypyrrole Nanoparticles

In previous part, we described the significant difference in rheological behaviors of the doped CPPY and the doped nPPY-(025CMCT) suspended in 4 wt% alginate. It seems that the rheological behaviors are governed by the competitive of inter-particles interaction versus the particle-polymer interaction (Cassagnau 2008). Since particle size implies the surface contact area of particles, therefore, the change in particle size may alter the rheological behaviors of the suspensions. To explore the effect of this parameter, different particle sizes of the doped nPPY, including 216 nm (nPPY025CMCT), 178 nm (nPPY05CMCT), and 136 nm (nPPY1CMCT), were synthesized and used to prepare the nPPY/alginate suspensions. The result of shear viscosity against shear rate is shown in Fig. 7.6. By

suspending 10 wt% of the different size of doped nPPY into 4 wt% alginate, the shear viscosity of the suspension monotonically deceases with decreasing the particle size of the doped nPPY (see Fig. 7.6a). This can be explained in that the smaller size nPPY creates a larger surface area to interact with alginate molecules resulting in more absorption of alginate on the surfaces of nPPY. As described previously, the interaction of the doped nPPY and alginate leads to the depletion of alginate concentration in the bulk medium. Moreover, the alginate-absorbed nPPY can stabilize in the medium and they are far apart from each other, at relatively low nPPY content (10 wt% nPPY), due to the electrostatic and the steric repulsions. Therefore, there is less possibility to form aggregation of those particles. Of course, the shear viscosity of suspensions apparently decreases with decreasing in the particle size.

However, the increasing in surfaces area of nPPY not only enhances the interaction of alginate and nPPY but it also enhances the inter-particles interaction of nPPY. The influence of inter-particles interaction is more pronounced at high nPPY content as shown in Figure 7.6b. By suspending 30 wt% nPPY content in 4 wt% alginate, the shear viscosity also decreases when the particles size of nPPY decreases form 217 nm to 178 nm. In contrast, when further decreases the particles size to 136 nm, the shear viscosity of the nPPY/alginate suspension turns increase. At relatively higher nPPY content (30 wt%), the inter-particles interaction, such as van der Waal attraction or electrostatic interaction, of the particles with larger surface area become more dominant because the particles get close together at higher nPPY content. This leads to the aggregation of particles and the result is an increase of suspension viscosity. However, the shear viscosity of all nPPY/alginate suspensions is still lower than that of neat alginate. Therefore, it indicated that the effect of particles-polymer interaction on rheological behaviors of the nPPY-(025CMCT)/alginate suspensions is more pronounced than the inter-particles interaction.

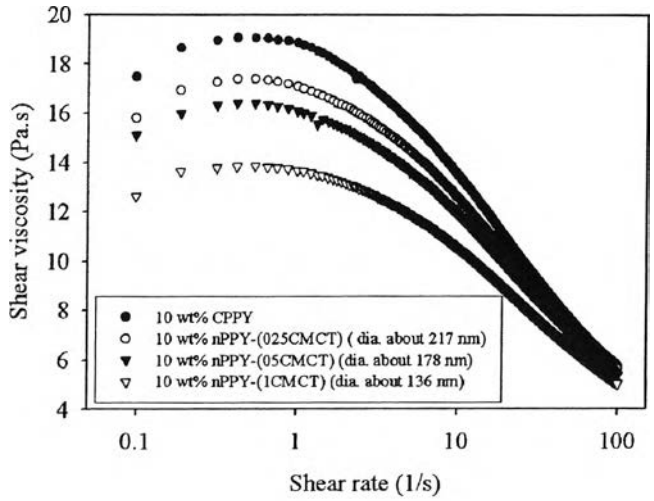

a

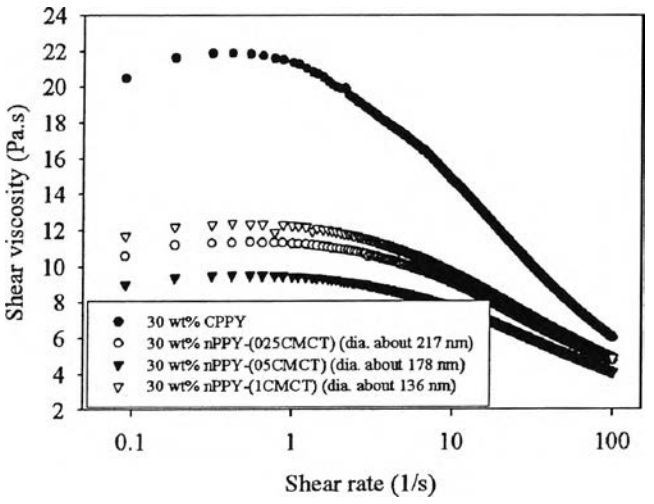

b

Figure 7.6 Plots of shear viscosity against shear rate of the different size of nPPY/alginate suspension with a) 10 wt% nPPY content and b) 30 wt% nPPY content.

7.4.3.3 Effect of Electronic States of Polypyrrole Nanoparticles

It is well known that the PPY have two electronic states, the conducting doped state with positive charge (oxidized state) and the insulating undoped state with no charge (neutral) (Geetha *et al.* 2006). Generally, the electronic states of PPY can be reversibly converted, without significant changes in morphology and particle size, by a chemical or an electrochemical method. To gain

insight some data on the interactions of different electronic states of PPY and alginate, rheological characterization was performed on suspensions containing the same amount of nPPY-(025CMCT), 10 and 30 wt%, in both doped and undoped states. In this present work, the undoped nPPY-(025CMCT) was obtained by the treatment of the doped nPPY-(025CMCT) with 0.5-M NaOH in order to achieve the particles with similar size and morphology. A substantial difference of shear viscosity of the nPPY/alginate suspensions is obtained, depending on the electronic states considered, as shown in Figure 7.7. As mentioned earlier, the shear viscosity of the doped nPPY-(025CMCT)/alginate suspensions decreases from the neat alginate with increasing the doped nPPY-(025CMCT) content from 10 to 30 wt% due to the depletion of alginate concentration in the bulk medium (see. Fig. 7.5a). On the other hand, by adding 10 wt% of the undoped nPPY-(025CMCT) to 4 wt% alginate, the shear viscosity is quite similar to that of neat alginate. However, the shear viscosity of the suspension significantly increases with increasing the undoped nPPY-(025CMCT) content up to 30 wt%. The increase in shear viscosity of the undoped nPPY/alginate is attributed to the aggregation of the undoped nPPY-(025CMCT) in alginate solution. In contrast to the doped nPPY-(025CMCT), the undoped nPPY-(025CMCT) has no charge to interact with negative charge alginate, hence prevent the absorption of alginate on surface of undoped nPPY-(025CMCT). Therefore, the depletion of alginate concentration in bulk medium and the stabilization of the undoped nPPY-(025CMCT) are hampered, while the inter-particle interactions of the undoped nPPY-(025CMCT) are more pronounced due to the enhancement of their hydrophobicity, compared to doped state. These result in the aggregation of the undoped nPPY-(025CMCT) and consequently increase of suspension viscosity.

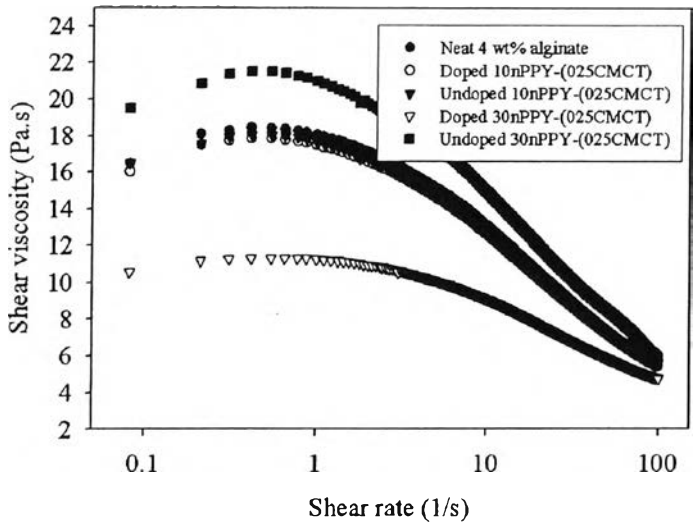

Figure 7.7 Plot of shear viscosity against shear rate of nPPY-(025CMCT)/alginate suspension with different electronic states of nPPY-(025CMCT).

7.4.3.4 Dynamic Light Scattering (DLS)

The dynamic light scattering (DLS) was used to determine hydrodynamic diameter of the synthesized nPPY, and the nPPY suspended in alginate. Table 7.1 exhibits the hydrodynamic diameter of the nPPY synthesized in the presence of different CM-chitin concentrations. It was observed that the mean diameters of the synthesized nPPY determined by dynamic light scattering measurement, those are 253 ± 3.88 nm for nPPY-(025CMCT), 201 ± 6.53 nm for nPPY-(05CMCT), and 161 ± 2.85 nm for nPPY-(1CMCT), are larger than those recognised from SEM images, those are 217 ± 17 nm for nPPY-(025CMCT), 178 ± 12 nm for nPPY-(05CMCT), and 136 ± 14 nm for nPPY-(1CMCT), respectively (see Fig. 7.1). DLS is used to determine the mean diameter of nPPY in aqueous media; therefore, the nPPY can be swollen. Of course, the hydrodynamic diameter of nPPY measured by DLS is slightly larger than that observed by SEM images, in which the nPPY is fully dried.

Table 7.1 Hydrodynamic diameter of the nPPY synthesized by using different concentration of CM-chitin

Sample	Mean diameter (nm)
Doped nPPY-(025CMCT)	253 ± 3.88
Doped nPPY-(05CMCT)	201 ± 6.53
Doped nPPY-(1CMCT)	161 ± 2.85

In addition, to determine the change in microstructure of nPPY in the presence of alginate, the hydrodynamic diameters of different nPPY contents suspended in alginate were measured as shown in Table 7.2. In this DLS measurement, the smallest particle sizes of both doped and undoped nPPY-(1CMCT) were used as representations. Again, the undoped nPPY-(1CMCT) was obtained by the treatment of doped nPPY1CMCT with 0.5-M NaOH. It is clearly found that diameter of the undoped nPPY1CMCT (163 nm) is quite similar to the doped nPPY1CMCT (161 nm). This confirms that the treatment of the doped nPPY-(1CMCT) with NaOH solution does not influence the particle size of the undoped nPPY-(1CMCT).

By suspending 10 wt% of the doped nPPY-(1CMCT) in alginate, the diameter of the doped nPPY-(1CMCT) is approximately 20% increased, compared to the original doped nPPY-(1CMCT). In addition, when increasing doped nPPY-(1CMCT) content in alginate up to 50 wt%, the obtained diameter is around 14% increase of the original ones. An increase in diameter is attributed to the absorption of alginate molecules on surfaces of the doped nPPY-(1CMCT) introduced by the electrostatic interaction between the opposite charges of nPPY-(1CMCT) and alginate.

In case of the undoped nPPY-(1CMCT)/alginate suspension, a 6% increase in diameter was observed at 10 wt% undoped nPPY-(1CMCT) in alginate. However, the change in diameter from original particles can be negligible when increased the undoped nPPY-(1CMCT) content up to 50 wt%. Since the

undoped nPPY-(1CMCT) has no charge to interact with alginate molecule, Therefore, these results indicate that the alginate molecules are more favorable absorbed on the surfaces of the doped nPPY-(1CMCT) than the undoped nPPY-(1CMCT). The DLS results provide a meaningful evident used to explain the different in rheological behaviors of doped and undoped nPPY in alginate suspensions, as described in previous parts.

Table 7.2 Hydrodynamic diameter of the synthesized nPPY-(1CMCT) suspended in alginate

Sample	Mean diameter (nm)	
	Doped form	Undoped form[a]
nPPY-(1CMCT)	161 ± 2.85	163 ± 1.23
10 wt% nPPY-(1CMCT/alginate	190 ± 2.05	173 ± 0.92
20 wt% nPPY-(1CMCT)/alginate	198 ± 2.23	175 ± 3.05
30 wt% nPPY-(1CMCT)/alginate	183 ±2.72	172 ± 0.99
40 wt% nPPY-(1CMCT)/alginate	184 ± 3.30	167 ± 3.50
50 wt% nPPY-(1CMCT)/alginate	184 ± 1.78	164 ± 4.67

[a] Undoped nPPY-(1CMCT) was obtained from the treatment of doped nPPY1CMCT with 0.5 M NaOH for 2 h.

7.5 Conclusion

In this paper, we synthesized the monodisperse spherical PPY nanoparticles (nPPY) by using CM-chitin as a template and, subsequently, investigated the rheological behaviors of the obtained PPY nanoparticles suspended in alginate solution compared to those of the conventional PPY macroparticles (CPPY). SEM images revealed that the different particle size of nPPY was obtained by varying the concentration of CM-chitin template. FTIR spectra indicated the identical structure of the synthesized nPPY and CPPY. When suspending the doped CPPY in alginate solution, the viscosity of the suspension increased with increasing PPY content. On the other hand, the addition of doped nPPY in alginate resulted in the decrease of viscosity of alginate. This could be explained in that the alginate could absorb on the surfaces of the doped nPPY due to the electrostatic interaction resulting in the depletion of alginate concentration in bulk medium as well as the decrease of chain entanglements of alginate molecules. Additionally, the stabilization of alginate-absorbed nPPY in alginate solution occurring from the electrostatic and steric repulsion of those particles also prevented the aggregation of nPPY. Combination of these two phenomenon resulted in the decrease of suspension viscosity. Moreover, it was further found that, by decreasing in size of nPPY, the viscosity decrease at low PPY content due to more favorable particles-polymer interaction of particles with larger surface area while the viscosity become increase when increase of PPY content due to the aggregation of particles at high PPY content. The viscosity of the suspension was clearly dependent on electronic states of nPPY. The incorporation of undoped nPPY in alginate increased the viscosity of suspension because poor absorption of alginate on surface of undoped nPPY, hence hampers the stabilization of undoped nPPY. Dynamic light scattering confirmed the variety in size of the synthesized nPPY and suggested that the alginate better absorbed on the surface of the doped nPPY than that of undoped nPPY.

7.6 Acknowledgements

The authors gratefully acknowledge the Thailand Research Fund (The Royal Golden Jubilee Ph.D. Program), the National Nanotechnology Center, The Conductive and Electroactive Polymers Research Unit, and Center for Petroleum, Petrochemicals, and Advanced Materials, Chulalongkorn University, Thailand, for their financial support of this work. We also acknowledge Surapon Food Public Co. Ltd. for supplying the material for this work.

7.7 References

Abu-Rabeaha, K. Marks, R.S. (2009) Impedance study of the hybrid molecule alginate–pyrrole: Demonstration as host matrix for the construction of a highly sensitive amperometric glucose biosensor. Sensors and Actuators B, 136, 516–522.

Baxter, A. Dillon, M. Taylor, K.D.A. (1992) Improved method for i.r. determination of the degree of N-acetylation of chitosan. International Journal of Biological Macromolecules, 14, 166-169.

Bhat, S.D. Mallikarjuna, N.N. Aminabhavi, T.M. (2006) Microporous alumino-phosphate (AlPO4-5) molecular sieve-loaded novel sodium alginate composite membranes for pervaporation dehydration of aqueous–organic mixtures near their azeotropic compositions. Journal of Membrane Science, 282, 473–483.

Brahim, S., Narinesingh, D., & Guiseppi-Elie, A. (2002). Bio-smart hydrogels: co-joined molecular recognition and signal transduction in biosensor fabrication and drug delivery. Biosensors and Bioelectronics, 17, 973–981.

Cassagnau, Ph. Melt rheology of organoclay and fumed silica nanocomposites. Polymer, 49, 2183-2196.

Chen K.L, Mylon SE, Elimelech M. (2006) Aggregation kinetics of alginate-coated hematite nanoparticles in monovalent and divalent electrolytes. Environmental Science and Technology. 40, 1516-1523.

Chen, K.L. Mylon, S.E. Elimelech, M. (2007) Enhanced aggregation of alginate-coated iron oxide (Hematite) nanoparticles in the presence of calcium, strontium, and barium cations. Langmuir, 23, 5920-5928.

Chen, S.A. Liao, C.S. (1993) Conductivity relaxation and chain motions in conjugated conducting polymers: neutral poly(3-alkylthiophenes). Macromolecules, 26, 2810-2816.

Dangtungee, R. Yun, J. Supaphol, P. (2005) Melt rheology and extrudate swell of calcium carbonate nanoparticle-filled isotactic polypropylene. Polymer Testing, 24, 2-11.

Doi, M. Kawaguchi, M. Kato, T. (2002) Rheology of fumed hydrophilic and hydrophobic titania suspensions dispersed in silicone oils. Colloids and Surfaces A: Physicochem. Eng. Aspects, 211, 223-231.

Einstein, A. (1906) On the theory of Brownian movement. Ann.Phys. (Leipz) 19. 371-381.

Geetha, S. Rao, C.R.K. Vijayan, M. Trivedi, D.C. (2006) Biosensing and drug delivery by polypyrrole. Analytica Chimica Acta, 568, 119–125.

Gombotz, W.R Wee, S.F. (1998) Protein release from alginate matrices. Advanced Drug Delivery Reviews, 31, 267-285.

He, F. Zhao, D. (2007) Manipulating the size and dispersibility of zerovalent iron nanoparticles by use of carboxymethyl cellulose stabilizers. Environmental Science and Technology, 41, 6216-6221.

Ismail, Y.A. Shin, K.M. Kim, S.J. (2009) A nanofibrous hydrogel templated electrochemical actuator: From single mat to a rolled-up structure. Sensors and Actuators B, 136, 438–443.

Ismail, Y.A. Shin, S.R. Shin, K.M. Yoon, S.G. Shon, K. Kim, S.I. Kim, S.J. (2008) Electrochemical actuation in chitosan/polyaniline microfibers for artificial muscles fabricated using an in situ polymerization. Sensors and Actuators B, 129, 834–840.

Kawakami, K. Nishihara, Y. Hirano, K. (2001) Effect of hydrophilic polymers on physical stability of liposome dispersions The Journal of Physical Chemistry B, 105, 2374–2385.

Kotwal, A. Schmidt, C.E. (2001) Electrical stimulation alters protein adsorption and nerve cell interactions with electrically conducting biomaterials. Biomaterials, 22, 1055-1064.

Krishnamoorti, R. Yurekli, K. (2001) Rheology of polymer layered silicate nanocomposites. Current Opinion in Colloid & Interface Science, 6, 464-470.

Kubo, W. Miyazaki, S. Attwood, D. (2003) Oral sustained delivery of paracetamol from in situ-gelling gellan and sodium alginate formulations, International Journal of Pharmaceutics, 258, 55-64.

Lattner, D. Flemming, H.C. Mayer, C. (2003) ^{13}C-NMR study of the interaction of bacterial alginate with bivalent cations. International Journal of Biological Macromolecules, 33, 81-88.

Li, X. Zhao, Y. Zhuang, T. Wang, G. Gu, Q. (2007) Self-dispersible conducting polyaniline nanofibres synthesized in the presence of β-cyclodextrin. Colloids and Surfaces A: Physicochem. and Eng. Aspects, 295, 146-151.

Liu, Q. Chen, D. (2008) Viscoelastic behaviors of poly(ε-caprolactone)/ attapulgite nanocomposites. European Polymer Journal, 44, 2046-2050.

Liu, X.X. Qian, L.Y. Shu, T. Tong, Z. (2003) Rheology characterization of sol–gel transition in aqueous alginate solutions induced by calcium cations through in situ release. Polymer, 44, 407–412.

Liu, Y. Chu, Y. Yang, L. (2006) Adjusting the inner-structure of polypyrrole nanoparticles through microemulsion polymerization. Materials Chemistry and Physics, 98, 304-308.

Mackey, M.E. Dao, T.T. Tuteja, A. Ho, D.L. Horn, B.V. Kim, H. Hawker, C.J. Nanoscale effects leading to non-Einstein-like decrease in viscosity. Nature Materials, 2, 762-766.

Mi, F.L. Chen, C.T. Tseng, Y.C. Kuan, CY. Shyu, S.S. (1997) Iron(III)-carboxymethylchitin microsphere for the pH-sensitive release of 6-mercaptopurine. Journal of Controlled Release, 44, 19-32.

Metzner A.B. (1989) Rheology of suspension in polymeric liquids. Journal of Rheology, 33, 421-454.

Niamlang, S. Sirivat, A. (2009) Electrically controlled release of salicylic acid from poly(p-phenylene vinylene)/polyacrylamide hydrogels. International Journal of Pharmaceutics. *in press*.

Okuzaki, H. Kondo, T. Kunugi, T. (1999) Characteristics of water in polypyrrole films. Polymer, 40, 995-1000.

Paitan, Y. Biran, D. Biran, I. Shechter, N. Babai, R. Rishpon, J. Ron, E.Z. (2003) On-line and in situ biosensors for monitoring environmental pollution. Biotechnology Advances, 22, 27–33.

Palma, R. Himmel, M.E. Brady, J.W. (2000) Calculation of the potential of mean force for the binding of glucose to benzene in aqueous solution. The Journal of Physical Chemistry B, 104, 7228-7234.

Pernaut, J.M. Reynolds, J.R. (2000) Use of conducting electroactive polymers for drug delivery and sensing of bioactive molecules, The Journal of Physical Chemistry B. 104, 4080–4090.

Peter, J. Hutter, W. Stoellnberger, W. Hampel, W.Detection of chlorinated and brominated hydrocarbons by an ion sensitive whole cell biosensor. Biosensors and Bioelectronics, 11 (1996) 1215–1219.

Salmon, M. Kanazawa, K.K. Diaz, A.F. Krounbi, M. (1982) A chemical route to pyrrole polymer films Journal of Polymer Science: Polymer Letters Edition, 20 187.

Sarvestani, A.S. (2008) Modeling the solid-like behavior of entangled polymer nanocomposites at low frequency regimes. European Polymer Journal, 44, 263–269.

Shen, Z. Chen, J. Zou, H. Yun, J. (2004) Rheology of colloidal nanosized $BaTiO_3$ suspension with ammonium salt of polyacrylic acid as a dispersant. Colloids and Surfaces A: Physicochem. Eng. Aspects, 244, 61-66.

Small, C. J. Too, C.O. Wallace, G.G. (1997). Responsive conducting polymer–hydrogel composites. Polymer Gels and Networks, 5, 251–265.

Sriamornsak, P. Thirawong, N. Korkerd, K. (2007) Swelling, erosion and release behavior of alginate-based matrix tablets. European Journal of Pharmaceutics and Biopharmaceutics, 66, 435-450.

Stejskal, J. Sapurina, I. (2004) On the origin of colloidal particles in the dispersion polymerization of aniline. Journal of Colloid and Interface Science. 274, 489-495.

Stenkamp, V.S. McGuiggan, P. Berg, J.C. (2001) Restabilization of electrosterically stabilized colloids in high salt media. Langmuir, 17, 637-651.

Thanpitcha, T. Sirivat, A. Jamieson, A.M. Rujiravanit, R. (2008) Dendritic polyaniline nanoparticles synthesized by carboxymethyl chitin templating. European Polymer Journal, 44, 3423–3429.

Thanpitcha, T. Sirivat, A. Jamieson, A.M. Rujiravanit, R. (2006) Preparation and characterization of polyaniline/chitosan blend film. Carbohydrate Polymers, 64, 560–568.

Tiller, C.L. O'Melia, C.R. (1993) Natural organic matter and colloidal stability: models and measurements. Colloids and Surfaces A: Physicochemical and Engineering Aspects, 73, 89-102.

Ueno, T, Yokota, S. Kitaoka, T. Wariishi, H. (2007) Conformational changes in single carboxymethylcellulose chains on a highly oriented pyrolytic graphite surface under different salt conditions. Carbohydrate Research, 342, 954-960.

Watthanaphanit, A. Supaphol, P. Tamura, H. Tokura, S. Rujiravanit, R. (2008) Fabrication, structure, and properties of chitin whisker-reinforced alginate nanocomposite fibers. Journal of Applied Polymer Science, 110, 890-899.

Wongpanit, P. Sanchavanakit, N. Pavasant, P. Supaphol, P. Tokura, S. Rujiravanit, R. (2005) Preparation and characterization of microwave-treated carboxymethyl chitin and carboxymethyl chitosan films for potential use in wound care application. Macromolecular Bioscience, 5, 1001-1012.

Xu, C. Willför, S. Holmlund, P. Holmbom, B. (2009) Rheological properties of water-soluble spruce O-acetyl galactoglucomannans. Carbohydrate Polymers, 75, 498–504.